

# Synthetic Counterfactual Labels for Efficient Conformal Counterfactual Inference

Amirmohammad Farzaneh

Matteo Zecchin

Oswaldo Simeone

KCLIP Lab, Centre for Intelligent Information Processing Systems (CIIPS)

Department of Engineering, King's College London, London, UK

Email: {amirmohammad.farzaneh, matteo.1.zecchin, osvaldo.simeone}@kcl.ac.uk

## Abstract

This work addresses the problem of constructing reliable prediction intervals for individual counterfactual outcomes. Existing conformal counterfactual inference (CCI) methods provide marginal coverage guarantees but often produce overly conservative intervals, particularly under treatment imbalance when counterfactual samples are scarce. We introduce synthetic data-powered CCI (SP-CCI), a new framework that augments the calibration set with synthetic counterfactual labels generated by a pre-trained counterfactual model. To ensure validity, SP-CCI incorporates synthetic samples into a conformal calibration procedure based on risk-controlling prediction sets (RCPS) with a debiasing step informed by prediction-powered inference (PPI). We prove that SP-CCI achieves tighter prediction intervals while preserving marginal coverage, with theoretical guarantees under both exact and approximate importance weighting. Empirical results on different datasets confirm that SP-CCI consistently reduces interval width compared to standard CCI across all settings.

## 1 Introduction

### 1.1 Context and Motivation

Consider a medical decision-making scenario in which a clinician must decide whether to administer a costly treatment, such as a new cancer therapy, to a patient. Each patient is characterized by a set of covariates  $X$ , e.g., demographics, medical history, and diagnostic test results, and may receive either the treatment ( $T = 1$ ) or no treatment ( $T = 0$ ). The observed outcome  $Y^{\text{obs}} = Y(T)$  could be a clinical metric such

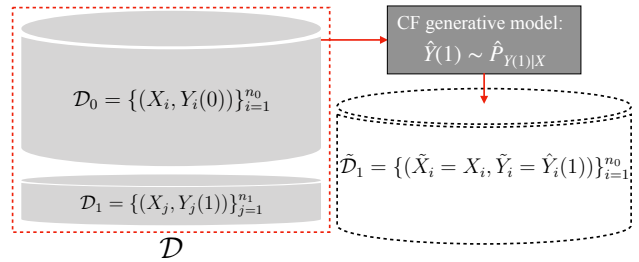


Figure 1: The proposed synthetic data-powered conformal counterfactual inference (SP-CCI) method leverages synthetic counterfactual labels  $\hat{Y}(1)$  produced using a pre-trained generative model  $\hat{P}_{Y(1)|X}$  from the, typically larger, dataset  $\mathcal{D}_0$  ( $n_0 \gg n_1$ ).

as tumor size reduction. The *counterfactual* outcome  $Y^{\text{cf}} = Y(1 - T)$  represents what would have happened had the patient received the other treatment option.

*Individual* counterfactual outcomes are fundamental to treatment effect estimation and policy evaluation. Clinicians are often interested not only in whether a new therapy outperforms standard care on average, but also in how much benefit it offers for a specific patient or for subgroups defined by covariates  $X$ . Achieving this goal requires quantifying uncertainty in predictions of the unobserved counterfactual outcome  $Y^{\text{cf}}$ . The challenge lies in the fundamental *missing data problem*: for each patient, only one of the potential outcomes ( $Y(0), Y(1)$ ), namely  $Y^{\text{obs}}$ , is observed, while the corresponding counterfactual outcome  $Y^{\text{cf}}$  is never directly available.

A promising solution to the problem of uncertainty quantification for individual counterfactual outcomes comes from *conformal prediction* [1, 2], a post-hoc calibration method that provides statistically valid prediction intervals without strong distributional assumptions. The recent technique introduced in [3], referred to here as *conformal counterfactual inference* (CCI), adapts conformal prediction to construct prediction

intervals for counterfactual outcomes with guaranteed marginal coverage. These guarantees hold regardless of the accuracy of the underlying predictive model.

CCI requires *calibration data* encompassing observations from the treatment arm whose outcome we wish to predict. However, in many medical datasets, treatment assignment is highly imbalanced: expensive or experimental treatments are administered only to a small fraction of patients, resulting in very few calibration samples for that arm [4]. As an illustration, in Fig. 1, the data set reporting the outcome  $Y(0)$ , corresponding to the control group, is larger than that reporting the treatment outcomes  $Y(1)$ .

Similar imbalances occur beyond medicine: in online advertising with sparse exposure to ad variants [5], in recommendation systems where many items lack interaction data [6], and in A/B testing where risky variants are shown to only a few users [7]. In all cases, scarce calibration data for the target arm yields wide, uninformative intervals, limiting CCI’s utility in high-stakes decisions.

A natural idea is to use *synthetic* counterfactual outcomes generated by a learned model, such as meta-algorithms for heterogeneous treatment effect estimation [8], causal forests [9], and deep structural causal models (DSCMs) [10]. Such models can produce plausible counterfactual outcomes for patients in the larger control group, increasing the effective calibration sample size for the treatment arm. In Fig. 1, the counterfactual (CF) generative model produces estimates  $\hat{Y}(1)$  for the counterfactual outcomes  $Y(1)$  of the control group. However, directly including the resulting synthetic data points in the CCI procedure breaks its statistical validity in terms of marginal coverage, since synthetic outcomes are biased approximations of the truth.

In this context, we propose *synthetic data-powered CCI* (SP-CCI), a conformal counterfactual inference framework that addresses the data imbalance problem by augmenting the calibration set with synthetic counterfactual labels, while preserving marginal coverage guarantees. SP-CCI integrates synthetic and real calibration data through a debiased miscoverage estimator informed by (i) prediction-powered inference (PPI) [11], which corrects for bias introduced by approximate labels and (ii) risk-controlling prediction sets (RCPS) [12], which choose the smallest interval widening that ensures the miscoverage risk is controlled with high probability. The result is a method that preserves CCI’s validity while improving its efficiency, yielding narrower prediction intervals, especially when high-quality synthetic counterfactual generators are available.

## 1.2 Further Related Work

**Counterfactual inference:** Counterfactuals and treatment effects can be estimated using meta-learners [8], representation learning [13], and architectures such as CFR/TARNet [14], as well as Bayesian and tree-based approaches like BART [15] and causal forests [9]. Generative models (e.g., CEVAE [16]) and structural causal models [10] learn latent structure for counterfactual estimation. All such methods provide point predictions rather than finite-sample, distribution-free intervals with coverage guarantees.

**Conformal prediction for counterfactuals:** Conformal inference has been adapted for counterfactuals in several ways: CCI [3], conformal sensitivity analysis [17], and conformal meta-learners for ITEs [18]. Despite differences in conformity scores and estimands, they all suffer in imbalanced settings, where calibration data scarcity yields wide intervals.

**Synthetic data in causal inference:** Generative models such as CEVAE [16], GANITE [19], and SCIGAN [20] impute missing counterfactuals, while model-based off-policy methods generate unobserved rewards for evaluation [6,21]. These approaches reduce variance but risk bias in conformal settings. Semi-supervised risk control via PPI [22] addresses bias correction by calibrating with model predictions. The proposed SP-CCI applies PPI to synthetic counterfactuals to provide statistical guarantees on counterfactual estimation.

## 1.3 Main Contributions

The main contributions of this work are summarized as follows.

- **Methodology:** We introduce SP-CCI, a conformal counterfactual inference method that combines real and synthetic calibration data via a debiased miscoverage estimator, ensuring valid high-probability coverage.
- **Theory:** We provide formal coverage guarantees under exact and approximate importance weighting, quantifying the effect of weight misspecification.
- **Applications:** We evaluate SP-CCI on synthetic data [3] and on the semi-synthetic IHDP dataset [15], showing consistent efficiency gains over CCI.

The rest of this paper is organized as follows. Sec. 2 formalizes the problem and sets up the notation. Sec. 3 reviews CCI and its limitations under treatment imbalance. Sec. 4 introduces the proposed SP-CCI method, along with theoretical guarantees. Sec. 5 presents empirical results on different datasets, and Sec. 6 concludes with a summary and discussion of future work.

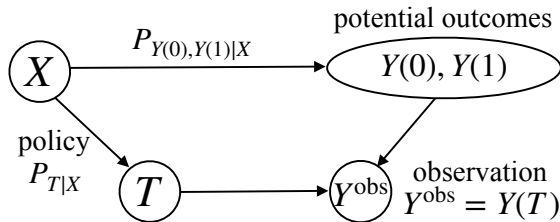


Figure 2: A Bayesian network representation of the observational setup for the potential outcomes framework under the SUTVA assumption and the strong ignorability assumption (2). The covariates  $X$  are correlated with the treatment through the assigned policy  $T \sim P_{T|X}$  and also with the potential outcomes  $(Y(0), Y(1)) \sim P_{Y(0), Y(1)|X}$ , with the observed outcome given by  $Y^{\text{obs}} = Y(T)$ . By the assumption (2), the treatment  $T$  is correlated with the potential outcomes  $(Y(0), Y(1))$  only through the covariates  $X$ .

## 2 Problem Definition

We consider the standard potential outcome framework for counterfactual inference with a binary treatment [23, 24]. Specifically, each unit  $i$  is associated with an observed covariate  $X_i \in \mathcal{X}$ , the pair of potential outcomes  $(Y_i(1), Y_i(0))$ , and a binary treatment assignment  $T_i \in \{0, 1\}$  determining the observed outcome  $Y_i^{\text{obs}}$ . Under the *stable unit treatment value assumption* (SUTVA) [25], the observed outcome  $Y_i^{\text{obs}}$  is the potential outcome under the treatment  $T_i$  and is given by  $Y_i^{\text{obs}} = Y_i(T_i)$ . The unobserved outcome  $Y_i^{\text{cf}}$ , also referred to as the *counterfactual* outcome, is the potential outcome under treatment not received, i.e.,  $Y_i^{\text{cf}} = Y_i(1 - T_i)$ . Thus, for each unit  $i$ , we observe the triplet  $(X_i, T_i, Y_i^{\text{obs}})$ , which includes only one of the potential outcome  $Y_i(T_i)$  corresponding to the treatment  $T_i$ .

We assume that the pair of potential outcomes, treatment, and covariate for each unit  $i$  are drawn independently and identically from a joint distribution  $P_{Y(0), Y(1), T, X}$ , i.e.,

$$(Y_i(1), Y_i(0), T_i, X_i) \stackrel{\text{i.i.d.}}{\sim} P_{Y(1), Y(0), T, X}. \quad (1)$$

Throughout, we adopt the standard assumption of *strong ignorability* [26–28]. This asserts that, under the given joint distribution in (1), the assigned treatment is conditionally independent of the potential outcomes given the covariates, i.e.,

$$P_{Y(1), Y(0), T|X} = P_{Y(1), Y(0)|X} P_{T|X}. \quad (2)$$

This assumption ensures that all relevant confounding factors are captured by the observed covariates, so that, after accounting for these covariates, the

treatment assignment is independent of potential outcomes and can be treated as randomized. A graphical representation of this conventional assumption via a Bayesian network is shown in Fig. 2 [29].

Given  $n$  units and the corresponding observed dataset  $\mathcal{D} = \{(X_i, Y_i^{\text{obs}} = Y_i(T_i), T_i)\}_{i=1}^n$ , the objective of this work is to reliably estimate the counterfactual outcome for a new unit by constructing prediction sets with marginal coverage guarantees. Without loss of generality, consider a test unit with treatment assignment  $T = 0$ . For this unit we observe  $(X, Y(0), T = 0)$ , and the target is the counterfactual outcome  $Y^{\text{cf}} = Y(1)$ . Our goal is to construct a prediction set  $\Gamma(X)$  for  $Y(1)$  such that

$$\Pr(Y(1) \in \Gamma(X)) \geq 1 - \alpha, \quad (3)$$

for some user-specified level  $1 - \alpha$ . By (3), the estimation set  $\Gamma(X)$  covers the true counterfactual  $Y(1)$  with probability no smaller than  $1 - \alpha$ .

To construct the set predictor  $\Gamma(X)$ , as in [3], we assume access to pre-trained quantile regressors  $\hat{q}_\gamma^0(X)$  and  $\hat{q}_\gamma^1(X)$ , which provide, respectively, estimates of the  $\gamma$ -quantiles, with  $\gamma \in [0, 1]$ , for the potential outcomes  $Y(0)$  and  $Y(1)$  associated with the covariates  $X$ . No assumption is made on the accuracy of these estimators, which can be designed using techniques such as quantile random forests [30], gradient-boosted quantile regression [31], or abductive inference via structural causal models (SCMs) [16, 32].

## 3 Background: Conformal Inference for Counterfactual Outcomes

To construct valid estimation sets  $\Gamma(X)$  for unobserved counterfactuals  $Y^{\text{cf}} = Y(1)$ , reference [3] proposed a method based on weighted conformal prediction (WCP). The method proposed by [3], referred to here as *conformal counterfactual inference* (CCI) leverages the pre-trained quantile regressor  $\hat{q}_\gamma^1(X)$  of the counterfactual outcome  $Y(1)$  given the covariates  $X$ . Henceforth, we use the simplified notation  $\hat{q}_\gamma(X) = \hat{q}_\gamma^1(X)$ . Furthermore, reference [3] assumes the *propensity score*

$$e(x) = \Pr(T = 1 | X = x), \quad (4)$$

i.e., the probability (obtained from the joint distribution (1)) of assigning treatment variable  $T = 1$  to a unit with covariates  $X$ , to be known. Additionally, it is assumed that the condition  $0 < e(x) < 1$ , known as the *overlap condition*, holds almost surely. Under these conditions, the following steps are applied:

**1. Split the calibration set by treatment:** Partition the calibration dataset  $\mathcal{D} = \{(X_i, Y_i(T_i), T_i)\}_{i=1}^n$

into the treatment-specific datasets

$$\begin{aligned} \mathcal{D}_0 &= \{(X_i, Y_i(0)) : T_i = 0\} \text{ and} \\ \mathcal{D}_1 &= \{(X_i, Y_i(1)) : T_i = 1\}, \end{aligned} \quad (5)$$

with sizes  $n_0$  and  $n_1$ , respectively, satisfying the equality  $n = n_0 + n_1$ .

**2. Compute the calibration nonconformity scores and importance weights:** For each point  $(X_i, Y_i(1))$  in the calibration dataset  $\mathcal{D}_1$ , using the pre-trained quantile regressor, compute the estimated quantiles  $\hat{q}_{\alpha_{\text{lo}}}(X_i)$  and  $\hat{q}_{\alpha_{\text{hi}}}(X_i)$  for the outcome  $Y_i(1)$ , where the probabilities  $\alpha_{\text{lo}}$  and  $\alpha_{\text{hi}}$  are selected to satisfy the equality  $1 - \alpha = \alpha_{\text{hi}} - \alpha_{\text{lo}}$ . Note that, if the regression model  $\hat{q}_\gamma(X)$  was perfectly accurate, the interval  $[\hat{q}_{\alpha_{\text{lo}}}(X_i), \hat{q}_{\alpha_{\text{hi}}}(X_i)]$  would include the true outcome  $Y_i(1)$  with probability  $1 - \alpha$ . However, the model is generally imperfect, and we can use the true label  $Y_i(1)$  to evaluate the estimation error as the *nonconformity score*

$$S_i = \max\{\hat{q}_{\alpha_{\text{lo}}}(X_i) - Y_i(1), Y_i(1) - \hat{q}_{\alpha_{\text{hi}}}(X_i), 0\}. \quad (6)$$

The score (6) equals zero if the outcome  $Y_i(1)$  is inside the estimated interval  $[\hat{q}_{\alpha_{\text{lo}}}(X_i), \hat{q}_{\alpha_{\text{hi}}}(X_i)]$ , and it increases as the observation gets further away from the estimated interval bounds. For each data point  $(X_i, Y_i(1)) \in \mathcal{D}_1$ , evaluate also the importance weight  $w_i = 1/e(X_i)$ .

**3. Evaluate the estimation set:** For a given test point  $X$  with  $T = 0$ , produce the estimation interval

$$\Gamma(X) = [\hat{q}_{\alpha_{\text{lo}}}(X) - \eta, \hat{q}_{\alpha_{\text{hi}}}(X) + \eta], \quad (7)$$

where the interval widening parameter  $\eta$  is computed as

$$\eta(X) = \inf \left\{ t \in \mathbb{R} : \frac{\sum_{i=1}^{n_1} \mathbf{1}(S_i \leq t) w_i}{\sum_{i=1}^{n_1} w_i + \frac{1}{e(X)}} \geq 1 - \alpha \right\}. \quad (8)$$

This selects the smallest value of  $\eta$  such that the empirical weighted coverage over the real calibration points, adjusted for the test point, reaches the target level  $1 - \alpha$ , thereby controlling the miscoverage rate at the desired level.

Reference [3] proves that the marginal guarantee (3) is satisfied by the estimation set (7) regardless of the accuracy of the quantile model  $\hat{q}_\gamma(X)$ . More precisely, the condition (3) is met by evaluating the probability over the joint distribution (1) of the calibration data  $\mathcal{D}$  used to compute the nonconformity scores and interval widening parameter  $\eta$ , as well as over the distribution of the test data point  $(X, T, Y(0))$  for which the estimation interval is constructed.

## 4 Efficient Conformal Inference with Synthetic Counterfactuals

The CCI approach reviewed in the previous section faces a key practical challenge [14]: there is often a significant imbalance in treatment assignment within observational datasets (see Fig. 1). In particular, the dataset  $\mathcal{D}_0$  encompassing data for untreated units can be much larger than the dataset  $\mathcal{D}_1$  for the treated units, i.e.,  $n_0 \gg n_1$ . For instance, in many medical applications, the number of treated units, i.e., with  $T = 1$ , is significantly smaller than the number of untreated ones, i.e., with  $T = 0$ . In fact, treatments are often costly or time-consuming to administer, while control data can be passively collected from existing records [33].

Given a test unit with treatment variable  $T = 0$ , the state-of-the-art CCI method constructs estimation intervals (7) for the counterfactual  $Y(1)$  using real treated data  $\mathcal{D}_1 = \{(X_i, Y_i) : T_i = 1\}$  as calibration data. When the dataset  $\mathcal{D}_1$  is small, the resulting intervals may become too wide to be useful. To address this limitation, in this section we introduce *synthetic data-powered CCI* (SP-CCI), which augments the calibration dataset  $\mathcal{D}_1$  with synthetic samples  $\tilde{\mathcal{D}}_1$  whose counterfactual labels are generated from the covariates of the larger control set  $\mathcal{D}_0$  (see Fig. 1). We use this augmented dataset to calibrate estimation intervals for the counterfactual outcome  $Y^{\text{cf}} = Y(1)$  that provide high-probability guarantees (3) on the miscoverage rate.

### 4.1 Generating Synthetic Counterfactual Labels

To augment the calibration dataset  $\mathcal{D}_1$  with synthetic data points generated from the dataset  $\mathcal{D}_0$ , we assume the availability of a counterfactual generative model  $\hat{P}_{Y(1)|X}$  pre-trained to approximately sample from the conditional distribution  $P_{Y(1)|X}$  of the outcome  $Y(1)$  given the covariates  $X$ . This model can be trained using standard methods such as the T-learner, S-learner, and X-learner [8]. By sampling from the model  $\hat{P}_{Y(1)|X}$ , we obtain the counterfactual label

$$\hat{Y}_1(X) \sim \hat{P}_{Y(1)|X}. \quad (9)$$

We also assume that the marginal treatment probability  $P_T$  is known. If this is not known a priori, it can be estimated from data, and the effect of an inaccurate estimation is studied in Sec. 4.3.

Using the synthetic counterfactuals, the synthetic calibration dataset  $\tilde{\mathcal{D}}_1$  is created as

$$\tilde{\mathcal{D}}_1 = \{(\tilde{X}_i, \tilde{Y}_i) = (X_i, \hat{Y}_i(1))\}_{i=1}^{n_0}, \quad (10)$$

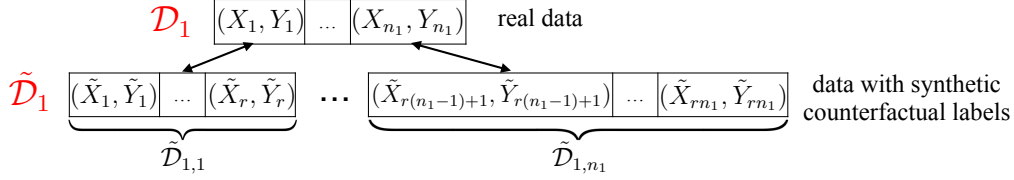


Figure 3: SP-CCI partitions the synthetic dataset  $\tilde{\mathcal{D}}_1$  into  $n_1$  disjoint groups  $\{\tilde{\mathcal{D}}_{1,i}\}_{i=1}^{n_1}$ , each with  $r$  data points. Each group  $\tilde{\mathcal{D}}_{1,i}$  is assigned to a real data point  $(X_i, Y_i)$  from the dataset  $\mathcal{D}_1$ .

where  $X_i$  represents the covariates for the  $i$ -th data point of dataset  $\mathcal{D}_0$ . As shown in Fig. 1, the dataset  $\tilde{\mathcal{D}}_1$  is thus derived from the factual dataset  $\mathcal{D}_0$  by assigning counterfactual labels to the covariates in dataset  $\mathcal{D}_0$  using the counterfactual generative model  $\hat{P}_{Y(1)|X}$ .

While this process effectively increases the size of the calibration dataset available for the treatment arm, it introduces a new challenge towards guaranteeing the coverage condition (3): the synthetic outcome  $\tilde{Y}_i$  in (10) is only an approximation of the corresponding true counterfactual outcome  $Y_i(1)$ . Therefore, simply merging the datasets  $\mathcal{D}_1$  and  $\tilde{\mathcal{D}}_1$  and applying the method in [3] to the resulting dataset would generally violate the coverage condition (3).

## 4.2 Constructing Reliable Estimation Sets using Synthetic Counterfactual Labels

Given a test point  $(X, T = 0)$ , in a manner similar to CCI (see (7)), we wish to construct an estimation interval  $\Gamma_\eta(X) = [\hat{q}_{lo}(X) - \eta, \hat{q}_{hi}(X) + \eta]$  for the counterfactual outcome  $Y(1)$ , where  $\hat{q}_{lo}(X)$  and  $\hat{q}_{hi}(X)$  are the estimated lower and upper quantile for the counterfactual  $Y(1)$  produced by the pre-trained model  $\hat{q}_\gamma(X)$ . Unlike CCI, the widening parameter  $\eta$  is calibrated to ensure that the coverage condition (3) by leveraging not only the smaller dataset  $\mathcal{D}_1$ , but also larger synthetic dataset  $\tilde{\mathcal{D}}_1$ .

To this end, using both datasets  $\mathcal{D}_1$  and  $\tilde{\mathcal{D}}_1$ , SP-CCI first obtains an unbiased estimate  $\hat{L}_\eta$  of the miscoverage probability  $L_\eta = \Pr(Y(1) \notin \Gamma_\eta(X))$ . Then, it evaluates an upper confidence bound  $\hat{L}_\eta^+$  on the probability  $L_\eta$  using the estimate  $\hat{L}_\eta$ . Finally, SP-CCI selects the parameter  $\eta$  so that the upper confidence bound  $\hat{L}_\eta^+$  does not exceed the target value  $\alpha$ . At a technical level, SP-CCI combines PPI [11], which is used to obtain the unbiased estimate  $\hat{L}_\eta$ , with RCPS [12], which supports the selection of the parameter  $\eta$ .

To elaborate, define the miscoverage loss for a given

widening parameter  $\eta$  and input-output pair  $(X, Y)$  as

$$\ell_\eta(X, Y) = \begin{cases} 0 & \text{if } Y \in [\hat{q}_{lo}(X) - \eta, \hat{q}_{hi}(X) + \eta], \\ 1 & \text{otherwise.} \end{cases} \quad (11)$$

The expectation of the loss (11) with respect to the distribution of the variables  $(X, Y(1))$  is given by the miscoverage probability

$$\begin{aligned} L_\eta &= \mathbb{E}[\ell_\eta(X, Y(1))] \\ &= \Pr(Y(1) \notin [\hat{q}_{lo}(X) - \eta, \hat{q}_{hi}(X) + \eta]) \\ &= \Pr(Y(1) \notin \Gamma_\eta(X)), \end{aligned} \quad (12)$$

which we wish to control according to the inequality in (3).

As mentioned, SP-CCI builds on an unbiased estimate  $\hat{L}_\eta$  of the expected loss (12) that incorporates both real and synthetic calibration sets. To construct this estimate, as illustrated in Fig. 3, we partition the  $n_0 > n_1$  examples in the dataset  $\tilde{\mathcal{D}}_1$  into  $n_1$  groups  $\{\tilde{\mathcal{D}}_{1,i}\}_{i=1}^{n_1}$  of  $r = \lfloor n_0/n_1 \rfloor$  data points each [22, 34]. Each group  $\tilde{\mathcal{D}}_{1,i} = \{(\tilde{X}_j, \tilde{Y}_j)\}_{j=r(i-1)+1}^{ri}$  is assigned to a different real calibration point  $(X_i, Y_i) \in \mathcal{D}_1$ .

Furthermore, SP-CCI computes the modified weights

$$w_i = \frac{P_{X_i}(X_i)}{P_{X_i|T}(X_i | 1)} = \frac{P_T(1)}{e(X_i)} \quad (13)$$

for all  $n_1$  real data points in dataset  $\mathcal{D}_1$ , and

$$\tilde{w}_i = \frac{P_{X_i}(\tilde{X}_i)}{P_{X_i|T}(\tilde{X}_i | 0)} = \frac{P_T(0)}{1 - e(\tilde{X}_i)} \quad (14)$$

for all  $n_0$  synthetic data points in dataset  $\tilde{\mathcal{D}}_1$ . Note that, unlike [3], the evaluation of the weights (13)-(14) requires knowledge not just of the propensity score  $e(\cdot)$ , but also of the treatment probability  $P_T(1)$ . The effect of a misspecified treatment probability  $p_T(1)$  is studied in Sec. 4.3.

Using the datasets  $\mathcal{D}_1$  and  $\tilde{\mathcal{D}}_1$ , SP-CCI constructs an estimate of the miscoverage probability (12) given by

$$\hat{L}_\eta = \frac{1}{n_1} \sum_{i=1}^{n_1} \hat{\ell}_{i,\eta}, \quad (15)$$

where  $\hat{\ell}_{i,\eta}$  is the estimate obtained using the  $i$ -th data point  $(X_i, Y_i)$  from the real dataset  $\mathcal{D}_1$ , as well as the corresponding group  $\tilde{\mathcal{D}}_{1,i} = \{(\tilde{X}_j, \tilde{Y}_j)\}_{j=r(i-1)+1}^{ri}$  from the synthetic dataset. Taking inspiration from PPI [11, 22, 34], this estimate is obtained as

$$\hat{\ell}_{i,\eta} = \frac{1}{r} \sum_{j=r(i-1)+1}^{ri} \tilde{w}_j \ell_\eta(\tilde{X}_j, \tilde{Y}_j) - w_i \left[ \ell_\eta(X_i, \hat{Y}_i) - \ell_\eta(X_i, Y_i) \right], \quad (16)$$

where  $\hat{Y}_i \sim \hat{P}_{Y(1)|X}$  represents an estimate of the outcome  $Y_i(1)$  corresponding to the covariate  $X_i$  in dataset  $\mathcal{D}_1$ .

The estimator (16) combines a (weighted) empirical estimate from synthetic data with a correction term derived from real data. Specifically, the first term in (16) averages the miscoverage loss over the  $r$  synthetic samples in group  $\tilde{\mathcal{D}}_{1,i}$ , which are scaled by their importance weights  $\tilde{w}_j$ . The second term adjusts for the potential bias in the synthetic counterfactual labels  $\tilde{Y}_j$  by subtracting an estimate of the bias. This estimate is obtained by computing the difference between the loss on the true outcome  $Y_i$  and its synthetic estimate  $\hat{Y}_i$ , which is scaled by weight  $w_i$ .

The quantity  $\hat{L}_\eta$  in (15) can be shown to be an unbiased estimator of the expected loss  $L_\eta$  (see Supplementary Material, Sec. 1). Furthermore, by Hoeffding's inequality, due to the fact that the terms  $\hat{\ell}_{i,\eta}$  are bounded in the interval  $[-1/\min_x\{e(x)\}, 1/\min_x\{e(x)\} + 1/(1 - \max_x\{e(x)\})]$  almost surely, we have the upper confidence bound on the miscoverage probability  $L_\eta$  [12]

$$\Pr \left( L_\eta \leq \hat{L}_\eta^+ = \hat{L}_\eta + C \sqrt{\frac{1}{2n_1} \log \left( \frac{1}{\delta} \right)} \right) \geq 1 - \delta \quad (17)$$

for any probability  $\delta$ , and  $C = 2/\min_x\{e(x)\} + 1/(1 - \max_x\{e(x)\})$ .

The estimation interval is finally given by

$$\Gamma(X) = \Gamma_{\hat{\eta}}(X) = [\hat{q}_{\text{lo}}(X) - \hat{\eta}, \hat{q}_{\text{hi}}(X) + \hat{\eta}], \quad (18)$$

where the widening parameter  $\hat{\eta}$  is selected so as to ensure that the upper bound  $\hat{L}_\eta^+$  on the miscoverage probability is within the target level  $\alpha$ , i.e., [22]

$$\hat{\eta} = \min \left\{ \eta \geq 0 : \hat{L}_\eta^+ \leq \alpha \right\}. \quad (19)$$

### 4.3 Theoretical Guarantees

In this section, we show that the proposed SP-CCI estimation set (18) satisfies the marginal coverage requirement (3) with probability no smaller than  $1 - \delta$ . We

first consider the case where the importance weights in (13) are known exactly, and then we analyze the impact of a mismatch between the weights used in (16) and the true weights (13)-(14). Note that mismatches in the weights may result from an imprecise knowledge of the treatment probability  $p_T(1)$ , even when the propensity score  $e(\cdot)$  is known.

**Proposition 1.** *For any test point  $(X, T = 0)$ , and for any probability  $0 < \delta < 1$ , the SP-CCI estimation interval  $\Gamma(X)$  in (18) satisfies the condition*

$$\Pr \left( \Pr \left( Y(1) \in \Gamma(X) \mid \mathcal{D}_1, \tilde{\mathcal{D}}_1 \right) \geq 1 - \alpha \right) \geq 1 - \delta, \quad (20)$$

where the inner probability is taken over the randomness of the test point  $(X, T = 0, Y(1))$ , while the outer probability is evaluated over the distribution of the calibration datasets  $\mathcal{D}_1$  and  $\tilde{\mathcal{D}}_1$  used to compute the estimation interval  $\Gamma(X)$ .

The next result shows that the coverage guarantee (20) can be retained even in the presence of a weight estimation error, as long as one suitably increases the widening parameter (19) to account for the quality of the estimated importance weights.

**Proposition 2.** *Let  $\hat{w}_i$  and  $\tilde{\hat{w}}_i$  denote estimates of the weights  $w_i$  and  $\tilde{w}_i$ , respectively, and assume that these estimates are used in lieu of the weights  $w_i$  and  $\tilde{w}_i$  in (16). Assume also that the estimated importance weights  $\hat{w}_i$  and  $\tilde{\hat{w}}_i$  satisfy the inequalities*

$$|\hat{w}_i - w_i| \leq \epsilon, \quad \text{and} \quad |\tilde{\hat{w}}_i - \tilde{w}_i| \leq \tilde{\epsilon} \quad (21)$$

for all data points for some  $\epsilon \geq 0$  and  $\tilde{\epsilon} \geq 0$ . Then, the SP-CCI estimation interval  $\Gamma(X)$  constructed using the estimated weights and with the widening parameter

$$\hat{\eta} = \min \left\{ \eta \geq 0 : \tilde{L}_\eta + \epsilon + \tilde{\epsilon} + \sqrt{\frac{1}{2n_1} \log \left( \frac{1}{\delta} \right)} \leq \alpha \right\} \quad (22)$$

satisfies the probabilistic guarantee (20), where  $\tilde{L}_\eta$  is calculated as in (15) by using the estimated weights  $\hat{w}_i$  and  $\tilde{\hat{w}}_i$  from (21).

## 5 Experiments

In this section, we empirically validate the proposed SP-CCI method and compare it against CCI through experiments on a synthetic dataset (Sec. 5.1) and a semi-synthetic dataset (Sec. 5.2)<sup>1</sup>. Additional experiments for a real-world dataset can be found in the supplementary material. We evaluate performance in terms of efficiency, measured by the size of the predicted intervals of the counterfactual estimates.

<sup>1</sup>The code for the experiments can be found at <https://anonymous.4open.science/r/SP-CCI-18F2>

## 5.1 Efficiency Advantages on Synthetic Data

We begin by evaluating SP-CCI on the same simulation setup used in [3].

**Data Generation:** Following [3, 9], let  $X' \in \mathbb{R}^{10}$  be a latent covariate vector  $X' \sim \mathcal{N}(0, \Sigma)$  distributed as a multivariate Gaussian with mean zero, unit variance, and equicorrelation  $\rho \in [0, 1]$  across all pairs of features. The observed covariates are squashed within the interval  $[0, 1]$  as  $X = \Phi(X')$ , where  $\Phi$  is the standard Gaussian cumulative distribution function, applied element-wise. Note that when  $\rho = 0$  the covariate vector  $X$  is uniformly distributed on the unit cube.

Treatment is assigned based solely on the first covariate  $X_1$ , according to the known propensity score model  $e(X) = 0.4\beta_{2,4}(X_1)$ , where  $\beta_{2,4}$  is the cumulative distribution function of the beta distribution with shape parameters  $(2, 4)$ . As in [3], we fix  $Y(0) = 0$  for all covariates  $X$ , and we assume the treated potential outcome  $Y(1)$  to be a noisy nonlinear function of the covariates as  $Y(1) = f(X_1) \cdot f(X_2) + \varepsilon$ , with  $f(x) = 2/(1 + \exp(-12(x - 0.5)))$  and  $\varepsilon \sim \mathcal{N}(0, 1)$ .

We generate a total of  $n = 5000$  samples  $(X, T, Y(0), Y(1))$  for each run. These samples are split into four disjoint parts: 30% of the data, denoted as  $\mathcal{D}_{\hat{q}}$ , is used to train the quantile regressors  $\hat{q}_\gamma(\cdot)$ ; another 30%, denoted by  $\mathcal{D}_{\hat{P}}$ , is used to train the counterfactual generative model  $\hat{P}_{Y(1)|X}$ ; 20%, denoted by  $\mathcal{D}_{\text{cal}}$ , is reserved as the calibration set to compute the widening parameter  $\eta$  in (22); and the remaining 20% form the test set  $\mathcal{D}_{\text{te}}$ .

To study the impact of the quality of synthetic labels on the performance of SP-CCI, we consider three counterfactual generative models trained on subsets of  $\mathcal{D}_{\hat{P}}$ . Specifically, we define: a low-quality (LQ) model, a medium-quality (MQ) model, and a high-quality (HQ) model trained on 20%, 60%, and 100% of the samples in  $\mathcal{D}_{\hat{P}}$ , respectively. We set the miscoverage requirement to  $\alpha = 0.15$  and the probability parameter in (20) to  $\delta = 0.1$ .

**Implementation:** The quantile regressor  $\hat{q}_\gamma(\cdot)$  is implemented as two separate gradient-boosted regression models [31] for  $\gamma = \alpha/2$  and  $\gamma = 1 - \alpha/2$ , using treated data points ( $T = 1$ ) from dataset  $\mathcal{D}_{\hat{q}}$  reserved for quantile estimation. We adopt the quantile loss, a learning rate of 0.1, and 500 boosting stages. The generative model  $\hat{P}_{Y(1)|X}$  is implemented as a neural network regressor, following the counterfactual imputation step in the X-learner framework [8].

**Results and discussion:** Fig. 4a shows the distribution of the empirical test marginal coverage rates for

CCI and SP-CCI across 50 runs over different random splits of the available dataset. By their respective theoretical properties, CCI meets the nominal coverage level of  $1 - \alpha = 0.85$  on average (dashed lines), while all SP-CCI variants meet this coverage level with a probability higher than  $1 - \delta = 0.9$ . Fig. 4b presents the corresponding distribution of the average test prediction interval width. The results demonstrate that SP-CCI consistently achieves narrower intervals compared to CCI, while still satisfying the coverage guarantee in (20). Furthermore, as the quality of the counterfactual generative model improves, from LQ to HQ, the interval width decreases, confirming that higher-quality synthetic data yields tighter and more informative prediction intervals.

## 5.2 Real-World Validation on the IHDP Dataset

We next validate SP-CCI on a semi-synthetic benchmark derived from the Infant Health and Development Program (IHDP), a widely used testbed for counterfactual inference [15]. In this dataset, covariates  $X \in \mathbb{R}^{25}$  represent real-world demographic and health-related attributes of premature infants and their mothers, such as birth weight, gestational age, and maternal education level. The potential outcomes  $Y(0)$  and  $Y(1)$  denote simulated measures of cognitive development under control and treatment, respectively, with the treatment corresponding to participation in an early childhood intervention program. In the original study, treatment was assigned at random, but reference [15] introduced selection bias by removing a non-random subset of treated units. This created a treatment-control imbalance, resulting in a dataset with a treated-to-control ratio of approximately one to four. We combine training and test dataset splits to form a pool of 1,746 data points, which we partition according to the same rules as in Sec. 5.1.

### Quantile estimation via deep structural causal models:

To estimate predictive intervals for the counterfactual outcome  $Y(1)$ , we adopt the deep structural causal model (DSCM) framework [10]. SCMs describe the generative process for the variables  $(Y(0), Y(1), T, X)$  in terms of a directed graph. In it, variables associated with child nodes are a deterministic function of the variables associated with the parent nodes and of a set of latent noise variables. SCMs support counterfactual inference via a sequence of *abduction*, *action*, and *prediction* steps [10]. Accordingly, once an SCM is established for variables  $(Y(0), Y(1), X, T)$ , a quantile estimation function  $\hat{q}_\gamma(\cdot)$  for the counterfactual observation  $Y(1)$  can be obtained via counterfactual inference.

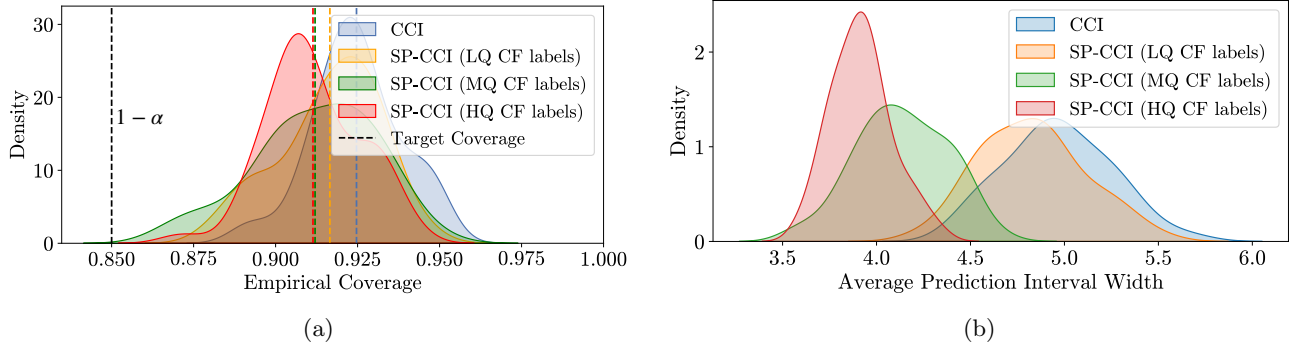


Figure 4: Synthetic data example from [3]: (a) Distribution of empirical test coverage for CCI [3] and SP-CCI (with counterfactual labels of different quality levels) evaluated over 50 independent realizations of the data. The black dashed line indicates the target level  $1 - \alpha = 0.85$ , while the other dashed lines represent the average empirical test coverage probabilities. (b) Distribution of the average test prediction interval width. (LQ/MQ/HQ: low-/medium-/high-quality; CF: counterfactual)

In our implementation, the observed variables  $(X, T, Y)$  are modeled as deterministic functions of latent exogenous noise variables via the SCM

$$X = f_X(Z_X), \quad T = f_T(X, Z_T), \quad Y = f_Y(X, T, Z_Y), \quad (23)$$

where  $Z_X, Z_T, Z_Y$  are mutually independent standard Gaussian vectors, and the functions  $f_X, f_T$ , and  $f_Y$  are implemented as neural networks. The neural networks in (23) are jointly trained with a variational inference model  $Q_{Z|X,T,Y}$ , whose role is to approximate the posterior distribution over the latent noise variables  $Z = (Z_X, Z_Y, Z_T)$  given observed data [10].

Given a test point  $(X, T = 0, Y^{\text{obs}})$ , we first perform abduction by drawing samples  $\hat{Z} \sim Q_{Z|X,T,Y}(Z | X, 0, Y^{\text{obs}})$ . Next, we take action by intervening to set  $T = 1$ , and finally we carry out prediction by evaluating  $f_Y(X, 1, \hat{Z}_Y)$ . Repeating this process with multiple samples  $\hat{Z}$  produces a distribution of counterfactual outcomes, from which we compute the empirical quantile  $\hat{q}_\gamma(X)$  using 100 Monte Carlo samples.

Note that, while the DSCM framework can be used for estimating the quantiles, it cannot be used as the counterfactual generative model for SP-CCI. This is due to the fact that the counterfactual generative model cannot be dependent on  $T$  in the debiasing step (16). As such, as in Sec. 5.1, the counterfactual generative model  $\hat{P}_{Y(1)|X}$  is implemented as a neural network regressor.

**Results and Discussion:** Table 1 reports the average width and standard error of the prediction intervals constructed using CCI and SP-CCI with varying synthetic data quality levels, obtained in the same way as Sec. 5.1. Consistent with our findings on synthetic data, SP-CCI produces significantly narrower intervals

than CCI, and the efficiency gains increase with the quality of the synthetic counterfactual generator.

Method	APIW	CVR
CCI	20.236	Not applicable
SP-CCI (LQ CF labels)	15.330	6%
SP-CCI (MQ CF labels)	14.562	4%
SP-CCI (HQ CF labels)	<b>14.240</b>	2%

Table 1: Average prediction interval width (APIW) and coverage violation rate (CVR) on the IHDP dataset for CCI [3] and SP-CCI evaluated over 50 independent realizations of the data. (LQ/MQ/HQ: low-/medium-/high-quality; CF: counterfactual)

## 6 Conclusion and Future Work

In this paper, we introduced SP-CCI, a synthetic data-powered extension of conformal counterfactual inference designed to address the efficiency limitations of CCI in imbalanced treatment settings. By augmenting the calibration set with synthetic counterfactual labels and applying a debiased miscoverage estimator inspired by PPI, SP-CCI achieves high-probability marginal coverage guarantees while producing substantially narrower prediction intervals. Theoretical analysis establishes robustness to importance weight misspecification, and experiments on various datasets demonstrate consistent efficiency gains over CCI.

Future work includes extending SP-CCI to also leverage synthetic data for calibrating the control group; the possibility of using counterfactual generative models conditioned on both covariates  $X$  and treatment  $T$  to better capture treatment-covariate interactions; and extending the framework to multi-arm and continuous treatments.

## Acknowledgments

This work was supported by the Open Fellowships of the EPSRC (EP/W024101/1) and by the EPSRC project (EP/X011852/1).

## References

- [1] Glenn Shafer and Vladimir Vovk. A tutorial on conformal prediction. *Journal of Machine Learning Research*, 9(3), 2008.
- [2] Vladimir Vovk, Alexander Gammernan, and Glenn Shafer. *Algorithmic learning in a random world*. Springer, 2005.
- [3] Lihua Lei and Emmanuel J Candès. Conformal inference of counterfactuals and individual treatment effects. *Journal of the Royal Statistical Society Series B: Statistical Methodology*, 83(5):911–938, 2021.
- [4] Issa J Dahabreh, Sarah E Robertson, Jon A Steingrimsdottir, Elizabeth A Stuart, and Miguel A Hernan. Extending inferences from a randomized trial to a new target population. *Statistics in medicine*, 39(14):1999–2014, 2020.
- [5] Léon Bottou, Jonas Peters, Joaquin Quiñero-Candela, Denis X Charles, D Max Chickering, Elon Portugaly, Dipankar Ray, Patrice Simard, and Ed Snelson. Counterfactual reasoning and learning systems: The example of computational advertising. *The Journal of Machine Learning Research*, 14(1):3207–3260, 2013.
- [6] Adith Swaminathan and Thorsten Joachims. Counterfactual risk minimization: Learning from logged bandit feedback. In *International conference on machine learning*, pages 814–823. PMLR, 2015.
- [7] Ron Kohavi, Diane Tang, and Ya Xu. *Trustworthy online controlled experiments: A practical guide to a/b testing*. Cambridge University Press, 2020.
- [8] Sören R Künnel, Jasjeet S Sekhon, Peter J Bickel, and Bin Yu. Metalearners for estimating heterogeneous treatment effects using machine learning. *Proceedings of the national academy of sciences*, 116(10):4156–4165, 2019.
- [9] Stefan Wager and Susan Athey. Estimation and inference of heterogeneous treatment effects using random forests. *Journal of the American Statistical Association*, 113(523):1228–1242, 2018.
- [10] Nick Pawlowski, Daniel Coelho de Castro, and Ben Glocker. Deep structural causal models for tractable counterfactual inference. *Advances in neural information processing systems*, 33:857–869, 2020.
- [11] Anastasios N Angelopoulos, Stephen Bates, Clara Fannjiang, Michael I Jordan, and Tijana Zrnic. Prediction-powered inference. *Science*, 382(6671):669–674, 2023.
- [12] Stephen Bates, Anastasios Angelopoulos, Lihua Lei, Jitendra Malik, and Michael Jordan. Distribution-free, risk-controlling prediction sets. *Journal of the ACM (JACM)*, 68(6):1–34, 2021.
- [13] Fredrik Johansson, Uri Shalit, and David Sontag. Learning representations for counterfactual inference. In *International conference on machine learning*, pages 3020–3029. PMLR, 2016.
- [14] Uri Shalit, Fredrik D Johansson, and David Sontag. Estimating individual treatment effect: generalization bounds and algorithms. In *International conference on machine learning*, pages 3076–3085. PMLR, 2017.
- [15] Jennifer L Hill. Bayesian nonparametric modeling for causal inference. *Journal of Computational and Graphical Statistics*, 20(1):217–240, 2011.
- [16] Christos Louizos, Uri Shalit, Joris M Mooij, David Sontag, Richard Zemel, and Max Welling. Causal effect inference with deep latent-variable models. *Advances in neural information processing systems*, 30, 2017.
- [17] Mingzhang Yin, Claudia Shi, Yixin Wang, and David M Blei. Conformal sensitivity analysis for individual treatment effects. *Journal of the American Statistical Association*, 119(545):122–135, 2024.
- [18] Ahmed M Alaa, Zaid Ahmad, and Mark van der Laan. Conformal meta-learners for predictive inference of individual treatment effects. *Advances in neural information processing systems*, 36:47682–47703, 2023.
- [19] Jinsung Yoon, James Jordon, and Mihaela Van Der Schaar. Ganite: Estimation of individualized treatment effects using generative adversarial nets. In *International conference on learning representations*, 2018.
- [20] Ioana Bica, James Jordon, and Mihaela van der Schaar. Estimating the effects of continuous-valued interventions using generative adversarial networks. *Advances in Neural Information Processing Systems*, 33:16434–16445, 2020.

- [21] Philip Thomas and Emma Brunskill. Data-efficient off-policy policy evaluation for reinforcement learning. In *International conference on machine learning*, pages 2139–2148. PMLR, 2016.
- [22] Bat-Sheva Einbinder, Liran Ringel, and Yaniv Romano. Semi-supervised risk control via prediction-powered inference. *arXiv preprint arXiv:2412.11174*, 2024.
- [23] Jerzy Splawa-Neyman, Dorota M Dabrowska, and Terrence P Speed. On the application of probability theory to agricultural experiments. essay on principles. section 9. *Statistical Science*, pages 465–472, 1990.
- [24] Donald B Rubin. Estimating causal effects of treatments in randomized and nonrandomized studies. *Journal of educational Psychology*, 66(5):688, 1974.
- [25] Donald B Rubin. Formal mode of statistical inference for causal effects. *Journal of statistical planning and inference*, 25(3):279–292, 1990.
- [26] Paul R Rosenbaum and Donald B Rubin. The central role of the propensity score in observational studies for causal effects. *Biometrika*, 70(1):41–55, 1983.
- [27] Donald B Rubin. Bayesian inference for causal effects: The role of randomization. *The Annals of statistics*, pages 34–58, 1978.
- [28] Guido W Imbens and Donald B Rubin. *Causal inference in statistics, social, and biomedical sciences*. Cambridge university press, 2015.
- [29] Daphne Koller and Nir Friedman. *Probabilistic graphical models: principles and techniques*. MIT press, 2009.
- [30] Nicolai Meinshausen and Greg Ridgeway. Quantile regression forests. *Journal of machine learning research*, 7(6), 2006.
- [31] Jerome H Friedman. Greedy function approximation: a gradient boosting machine. *Annals of statistics*, pages 1189–1232, 2001.
- [32] Judea Pearl. *Causality*. Cambridge university press, 2009.
- [33] Daniele Ballinari. Calibrating doubly-robust estimators with unbalanced treatment assignment. *Economics Letters*, 241:111838, 2024.
- [34] Sangwoo Park, Matteo Zecchin, and Osvaldo Simeone. Adaptive prediction-powered autoeval with reliability and efficiency guarantees. *arXiv preprint arXiv:2505.18659*, 2025.
- [35] Benedikt Koch and Kosuke Imai. Statistical decision theory with counterfactual loss. *arXiv preprint arXiv:2505.08908*, 2025.
- [36] Sara Khosravi, Hossein Shokri-Ghadikolaie, and Marina Petrova. Learning-based handover in mobile millimeter-wave networks. *IEEE Transactions on Cognitive Communications and Networking*, 7(2):663–674, 2020.
- [37] Jakob Hoydis, Sebastian Cammerer, Fayçal Ait Aoudia, Avinash Vem, Nikolaus Binder, Guillermo Marcus, and Alexander Keller. Sionna: An open-source library for next-generation physical layer research. *arXiv preprint arXiv:2203.11854*, 2022.

## Synthetic Counterfactual Labels for Efficient Conformal Counterfactual Inference: Supplementary Materials

### A Proofs

**Proposition 3.** *The quantity  $\hat{L}_\eta$  defined in (15) is an unbiased estimator of the expected loss  $L_\eta$  in (12).*

*Proof.* Recall from (15) and (16) that

$$\hat{L}_\eta = \frac{1}{n_1} \sum_{i=1}^{n_1} \left( \frac{1}{r} \sum_{j=r(i-1)+1}^{ri} \tilde{w}_j \ell_\eta(\tilde{X}_j, \tilde{Y}_j) - w_i [\ell_\eta(X_i, \hat{Y}_i) - \ell_\eta(X_i, Y_i)] \right),$$

where each  $(\tilde{X}_j, \tilde{Y}_j)$  is drawn from  $\tilde{\mathcal{D}}_1$ , and each  $(X_i, Y_i)$  from  $\mathcal{D}_1$ .

Taking the expectation over all data-generating randomness, and using linearity of expectation, we obtain

$$\mathbb{E}[\hat{L}_\eta] = \frac{1}{n_1} \sum_{i=1}^{n_1} \left( \frac{1}{r} \sum_{j=r(i-1)+1}^{ri} \mathbb{E} [\tilde{w}_j \ell_\eta(\tilde{X}_j, \tilde{Y}_j)] - \mathbb{E} [w_i \ell_\eta(X_i, \hat{Y}_i)] + \mathbb{E} [w_i \ell_\eta(X_i, Y_i)] \right). \quad (24)$$

Now, by the definitions of the importance weights in (13)–(14), we have the identities

$$\mathbb{E} [\tilde{w}_j \ell_\eta(\tilde{X}_j, \tilde{Y}_j)] = \mathbb{E}_{p(X, \hat{Y}(1))} [\ell_\eta(X, \hat{Y})], \quad (25)$$

$$\mathbb{E} [w_i \ell_\eta(X_i, \hat{Y}_i)] = \mathbb{E}_{p(X, \hat{Y}(1))} [\ell_\eta(X, \hat{Y})], \quad (26)$$

$$\mathbb{E} [w_i \ell_\eta(X_i, Y_i)] = \mathbb{E}_{p(X, Y(1))} [\ell_\eta(X, Y(1))] = L_\eta. \quad (27)$$

Substituting these into (24), and noting that the first two terms cancel exactly, we get:

$$\mathbb{E}[\hat{L}_\eta] = L_\eta.$$

Hence,  $\hat{L}_\eta$  is an unbiased estimator of  $L_\eta$ . □

*Proof of Proposition 1.* Combining (17) and (19), and given (12), we have

$$\Pr(\Pr(Y(1) \notin [\hat{q}_{\text{lo}}(X) - \eta, \hat{q}_{\text{hi}}(X) + \eta]) \leq \alpha) \geq 1 - \delta. \quad (28)$$

which is the same as condition (20). □

*Proof of Proposition 2.* Given that all the terms in (16) by which the weights get multiplied are in the interval  $[-1, 1]$ , we obtain

$$\left| \mathbb{E}[\tilde{L}_\eta] - \bar{\ell}_\eta \right| \leq \epsilon + \tilde{\epsilon}, \quad (29)$$

where  $\tilde{L}_\eta$  is calculated as in (15) by using the estimated weights  $\hat{w}_i$  and  $\hat{\tilde{w}}_i$  from (21). Consequently, the guarantee (20) still holds as long as the widening parameter  $\hat{\eta}$  is chosen as per (22). □

## B Algorithmic Properties and Complexity of SP-CCI

We analyze SP-CCI in terms of time and space complexity. Denote by  $C_q$  the cost of a single evaluation of the pre-trained quantile functions  $\hat{q}_{\alpha_{lo}}(\cdot)$ ,  $\hat{q}_{\alpha_{hi}}(\cdot)$ , and by  $C_{\text{gen}}$  the cost of drawing one synthetic counterfactual label from  $\hat{P}_{Y(1)|X}$ . Models are treated as fixed (training costs are listed separately).

**Monotonicity and search over  $\eta$ :** For each data point  $(x, y)$ , define the threshold

$$s(x, y) = \max\{\hat{q}_{\alpha_{lo}}(x) - y, y - \hat{q}_{\alpha_{hi}}(x), 0\},$$

i.e., the smallest widening  $\eta$  for which the interval  $[\hat{q}_{\alpha_{lo}}(x) - \eta, \hat{q}_{\alpha_{hi}}(x) + \eta]$  covers  $y$ . Then the miscoverage indicator equals  $\ell_\eta(x, y) = \mathbb{1}\{s(x, y) > \eta\}$ . Consequently, the debiased empirical miscoverage  $\hat{L}_\eta$  in (15)–(16) is a right-continuous, nonincreasing, piecewise-constant function of  $\eta$ , and it can only change at the thresholds

$$\{s(\tilde{X}_j, \tilde{Y}_j)\}_{j=1}^{n_0} \cup \{s(X_i, Y_i)\}_{i=1}^{n_1} \cup \{s(X_i, \hat{Y}_i)\}_{i=1}^{n_1},$$

where  $\hat{Y}_i \sim \hat{P}_{Y(1)|X}(\cdot | X_i)$  are the imputed treated outcomes used in the PPI correction term of (16). Therefore, there are at most  $m = n_0 + 2n_1$  candidate change-points. To find the smallest  $\hat{\eta}$  with  $\hat{L}_\eta^+ \leq \alpha$ , it suffices to sort these  $m$  thresholds and scan once with cumulative (importance) weights, yielding  $\mathcal{O}(m \log m)$  time for this step.

**Calibration-time time complexity:** We decompose calibration into four steps:

1. *Synthetic label generation:* build  $\tilde{\mathcal{D}}_1$  by drawing  $\tilde{Y}_j \sim \hat{P}_{Y(1)|X}(\cdot | \tilde{X}_j)$  for all  $j \leq n_0$ , and draw one  $\hat{Y}_i \sim \hat{P}_{Y(1)|X}(\cdot | X_i)$  for each  $i \leq n_1$  (used in the debiasing term of (16)):

$$T_{\text{gen}} = \mathcal{O}((n_0 + n_1)C_{\text{gen}}).$$

2. *Quantile evaluations:* evaluate  $\hat{q}_{\alpha_{lo}}$  and  $\hat{q}_{\alpha_{hi}}$  at all covariates in  $\tilde{\mathcal{D}}_1 \cup \mathcal{D}_1$ :

$$T_q = \mathcal{O}((n_0 + n_1)C_q).$$

3. *Precompute thresholds and weights:* compute  $s(\tilde{X}_j, \tilde{Y}_j)$  for  $j \leq n_0$ , and  $s(X_i, Y_i)$ ,  $s(X_i, \hat{Y}_i)$  for  $i \leq n_1$ ; compute importance weights via (13)–(14):

$$T_{\text{prep}} = \mathcal{O}(n_0 + n_1).$$

4. *Select  $\hat{\eta}$ :* sort the  $m = n_0 + 2n_1$  thresholds and scan once with cumulative weights to find the smallest  $\hat{\eta}$  satisfying  $\hat{L}_\eta^+ \leq \alpha$ :

$$T_{\text{sort}} = \mathcal{O}(m \log m).$$

Putting the steps together,

$$T_{\text{cal}} = \mathcal{O}((n_0 + n_1)(C_q + C_{\text{gen}}) + (n_0 + 2n_1) \log(n_0 + 2n_1)).$$

In typical neural implementations,  $C_q$  and  $C_{\text{gen}}$  (model forward passes) dominate the log factor.

**Test-time time complexity:** For a test covariate  $X$  with  $T = 0$ , SP-CCI outputs  $\Gamma(X) = [\hat{q}_{\alpha_{lo}}(X) - \hat{\eta}, \hat{q}_{\alpha_{hi}}(X) + \hat{\eta}]$ , requiring only two quantile evaluations:

$$T_{\text{test}} = \mathcal{O}(C_q).$$

**Space complexity:** We store the  $m = n_0 + 2n_1$  thresholds and their weights, plus optional cumulative arrays for the scan. Consequently, the space complexity can be calculated as

$$S = \mathcal{O}(n_0 + n_1),$$

in addition to constant-size model parameters. A streaming grid-search variant (without sorting) trades increased time for reduced peak memory.

**Training costs (one-off):** SP-CCI assumes pre-trained models:

- Quantile regressors  $\hat{q}_\gamma(\cdot)$ : training cost  $T_{\text{train}}^{(q)}$  (e.g., gradient-boosted quantile regression or DSCM-based quantiles).
- Counterfactual generator  $\hat{P}_{Y(1)|X}$ : training cost  $T_{\text{train}}^{(\text{gen})}$  (e.g., a regression network as in the X-learner imputation step).

These are standard supervised-learning costs on their respective splits and are not part of the conformal calibration time.

**Computing infrastructure:** All experiments were carried out on a local workstation (Apple MacBook Pro, Apple M1 Pro CPU, 16 GB unified memory). No external GPUs or cloud resources were used.

## C Policy Evaluation via Counterfactual Loss

Classical statistical decision theory evaluates a policy solely based on observed outcomes. However, such standard loss functions are inherently limited in that they cannot assess how much better, or worse, a different decision might have been. An example of alternative performance measures is given by the regret, which is used in online optimization to evaluate the performance gap with respect to an optimal policy. The framework of *counterfactual loss* introduced in [35] generalizes the notion of regret by allowing for the quantification of the quality of a decision using all potential outcomes. In this framework, we demonstrate the use of synthetic counterfactual labels via SP-CCI for policy evaluation with respect to counterfactual losses.

A policy  $\pi_\theta : \mathcal{X} \rightarrow \{0, 1\}$  with hyperparameter  $\theta$  maps covariates  $X$  to a binary decision  $T \in \{0, 1\}$ . The counterfactual loss associated with a decision  $\pi_\theta(X)$  is a function  $\ell(\pi_\theta(X); Y(0), Y(1))$  that evaluates not just the observed outcome  $Y(\pi_\theta(X))$ , but also the unobserved alternative  $Y(1 - \pi_\theta(X))$  [35]. For example, as mentioned, if the outcome  $Y(T)$  represents a measure of reward, the *regret*,

$$\ell(\pi_\theta(X); Y(0), Y(1)) = Y(1 - \pi_\theta(X)) - Y(\pi_\theta(X)), \quad (30)$$

is a counterfactual loss, measuring the gap between the reward that could have been obtained,  $Y(1 - \pi_\theta(X))$ , and the actual reward  $Y(\pi_\theta(X))$ .

**Experimental setup and data generation:** We consider a setting of practical engineering relevance, namely handover in wireless cellular systems [36]. As illustrated in Fig. 5, given the location  $X \in \mathbb{R}^3$  of a mobile device, the policy  $\pi_\theta(\cdot)$  connects the user to one of two base stations (BSs) in the proximity of the device. The observed outcome  $Y^{\text{obs}} = Y(T)$  denotes the received signal strength at the selected BS  $T = \pi_\theta(X)$ , while the unobserved counterfactual outcome  $Y^{\text{cf}} = Y(1 - T)$  is the signal strength that would have been received by the other BS.

We generate a dataset of 2,000 data points  $(Y(0), Y(1), T, X)$  by leveraging the ray tracing tool Sionna [37] on uniformly selected locations within the *Place de l'Étoile* environment [37]. We wish to evaluate the performance of a conventional policy  $\pi_\theta(\cdot)$  that deterministically assigns the treatment, i.e., BS,  $T$ . In the generated dataset, we assume that only the outcome from one treatment is observed, which in this case is the BS that results in the highest received power by the user. The dataset is split into five equal partitions for training quantile models, training counterfactual estimators, calibration, policy optimization, and final evaluation.

**Policy optimization via counterfactual inference:** We wish to evaluate the performance of a family of threshold-based handover policies of the form  $\pi_\theta(X) = \mathbb{I}\{s(X) > \theta\}$ , where  $s(X)$  is a scalar summary of the mobile location  $X$ , and  $\theta$  is a tunable threshold. For each threshold  $\theta$ , the policy assigns BS 1 to instances where  $s(X) > \theta$ , and BS 0 otherwise. The performance of policy  $\pi_\theta(\cdot)$  is assessed using the average regret in (30). Specifically, for each threshold  $\theta$ , we evaluate a prediction interval for the regret (30), as we only have the outcome from the observed treatment, and report the lower bound or the upper bound of the estimation interval as sound pessimistic and optimistic estimates, respectively, of the policy's performance.

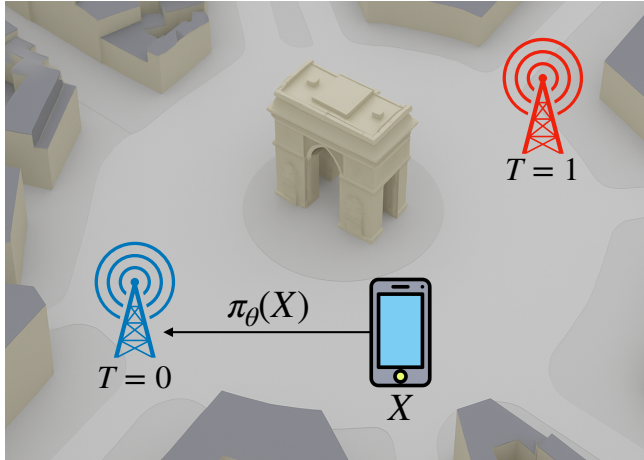


Figure 5: Policy evaluation for counterfactual loss in a wireless handover setting: A mobile device at location  $X \in \mathbb{R}^3$  is assigned to a BS indexed by  $T \in \{0, 1\}$  by a policy  $\pi_\theta(X)$ . The counterfactual loss (30) measures the difference between the signal strength that could have been obtained  $Y(1 - \pi_\theta(X))$ , and the actual reward  $Y(\pi_\theta(X))$ .

**Results and discussion:** We compare the average width of prediction intervals obtained using CCI and SP-CCI across 50 trials for a fixed policy threshold  $\theta = 80$ . As seen in Fig. 6, SP-CCI yields consistently narrower intervals, suggesting more precise performance quantification for a given fixed policy. Since the received powers in our dataset are measured in dBm, the reported interval widths are also expressed in dB.

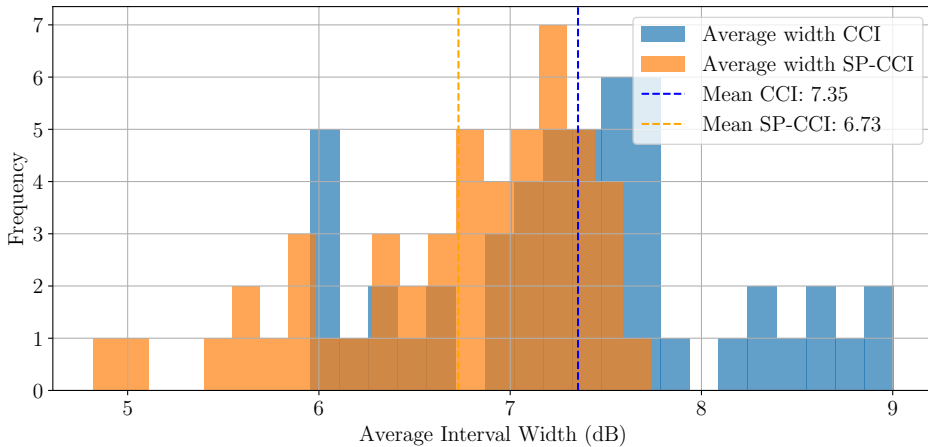


Figure 6: Distribution of average interval widths (in dB) over 50 random trials for optimistic CCI and SP-CCI methods, using a fixed policy threshold  $\theta = 80$ . Dashed lines indicate the average value of the distribution.